Investigation of Influence of Compact Actuators on Air Cavity in Water Flow

under Recessed Hull

Jeffrey M. Collins and Konstantin I. Matveev¹

School of Mechanical and Materials Engineering, Washington State University, Pullman, WA, 99163, USA

ABSTRACT

Air cavity drag reduction is one promising method for reducing power consumption of ships. Its current

practical applications are rather limited, owing largely to the fact that air cavity size and shape change

drastically in response to variations in ship attitude, motions and speed, as well as sea conditions. This

study explores how deployment of moveable hydrodynamic actuators near the air cavity on a small-

scale simplified hull form can effectively increase the air cavity size in adverse hull positions.

Experimentally investigated actuators included an adjustable plate in the front part of an air cavity, a

stern spoiler, and a hydrofoil with regulated attack angle and streamwise position beneath the hull. In

the cases of significant hull trims that are challenging for maintenance of long air cavities, optimal

actuator placement increased cavity length by nearly 110% from its degraded state at negative trim and

by 24% at positive trim. Actuator effects were more pronounced at higher water speeds.

Key words: Air-ventilated water flow; air cavity ship; hydrofoil; flow manipulation.

¹ Corresponding author. Email: matveev@wsu.edu

1

1. INTRODUCTION

consumption or higher top speeds, depending on the application. Air lubrication is a proven way to reduce friction drag, although limited experimental data and lack of confidence in computational fluid dynamics (CFD) prediction for this type of flow inhibit wide commercial adoption of the technology. A small number of ships have successfully used air lubrication. For example, fuel savings up to 15% were reported for inland waterway ferries employing a novel air-based drag reduction system [1]. Potential fuel savings are estimated to reach 20-30% when optimized systems are developed [2,3], though maintaining high performance in a broad range of operational conditions requires further R&D efforts. The concept of air lubrication has been around for well over a century, with early patents dating back to 1890 [4]. Modern experiments have shown that different methods for implementing air lubrication result in very different drag-altering phenomena, prompting further categorization of techniques shown schematically in Fig. 1. While terminology varies between researchers, the primary differences occur between a continuous injection of small bubbles, known as bubble drag reduction (BDR), the formation of a thin air layer along the ship hull, known as air layer drag reduction (ALDR), and the use of a specially designed recess and/or initiating wedge to help form and stabilize an air cavity, known as air cavity drag reduction (ACDR). The physics of BDR is rather complex, details of which were recently reviewed in [5]. ALDR can provide higher drag reduction than BDR, but the layer is easily disturbed and requires larger

Reducing water friction drag has favorable effects on ship power requirements, resulting in lower fuel

ACDR performance depends heavily on the geometry of the air cavity recess, which influences cavity formation and stability. Both of these factors govern the required airflow rates needed to achieve drag

rates of air injection [6]. ACDR, which is the primary focus of this study, is more stable in the presence of

flow disturbances and can yield greater drag reduction with less air injection than ALDR [7], but requires

more substantial modifications of the hull geometry.

saving effects and the subsequent power consumption by the air supply system, in turn defining net power savings of the ship [7]. Previous studies have shown that establishing an air cavity can require 3-5 times the airflow needed to maintain a stable cavity after formation [8,9]. Hence, maintaining a stable cavity will reduce the overall pumping power consumed by the air supply system and increase net power savings of the system.

The most prominent feature of ACDR systems is a backward-facing step or wedge located on the ship hull, as shown in Fig. 1c. Air cavity studies conducted on a flat plate under various flow conditions demonstrated that lower rates of air injection were possible with the inclusion of a step, while the cavity exhibited greater stability in the presence of water flow disturbances [2]. The maximum length of a cavity formed behind a wedge on a horizontal surface is known to be limited by the presence of waves at the air-water interface [10]. In calm water, a wavelength of the simplest transverse wave generated by an object moving with velocity U can be calculated as follows,

$$\lambda = \frac{2\pi U^2}{g} \tag{1}$$

where g is the gravity constant. For a stepped hull surface, the maximum or limiting cavity length $L_{c,lim}$ was estimated by potential flow theory as follows [11],

$$L_{c,lim} \approx 0.37\lambda$$
 (2)

The rate of air supply required to maintain a stable cavity must equal the rate of air leakage, which is affected by re-entrant water jets and bubbly zones at the cavity tails at sufficiently large Reynolds numbers [9,12]. Air leakage can be reduced by adding a sloping "beach" near the expected cavity closure location, which can also allow its length to exceed the limiting case of Eq. (2) and instead form a single cavity with a multi-wave interface, as shown in Fig. 2. Experiments have demonstrated that the beach adds pressure drag when wetted, thus requiring the cavity to maintain its maximum possible length for optimal drag reduction [8,13].

The limiting parameters of an air cavity under ideal conditions were previously identified using inviscid potential flow theory [11]. These models related the height of a wedge or step, water speed, cavity pressure, and cavity length to the closure angle of the tail. The results were used to select the step height and beach angle for previously mentioned ACDR experiments [8]. The potential flow model suggested that additional improvements of cavity length could be achieved using stern attachments to block downstream air leakage and hydrofoils positioned near the air-water interface. Hydrofoils were also predicted to have positive effects on air cavity behavior in potential flow models [11], and have been frequently used on fast boats in the past to provide lifting force on the hull and improve hydrodynamics [14]. Some limited experiments have verified that a properly placed hydrofoil can expand air cavity size in conditions where cavity degradation was present [15]. Predicting hydrofoil performance near a free surface can be difficult due to effects of cavitation, air entrainment, and free surface deformations. The understanding and modeling of hydrofoil interactions with an air cavity requires further research.

Hulls of fast displacement and planing boats can sometimes benefit from the addition of stern appendages such as wedges, flaps, and interceptors. Experiments performed by the US Navy demonstrated that their use can reduce drag for large destroyer vessels [16], while similar trim tabs are also applied for optimizing attitudes of small fast-moving ships. The ability of similar appendages to slow air leakage from ACDR systems has been predicted but not yet verified [11], although similar devices have been used block air pockets from moving downstream in storm drains [17].

Changes in the hull trim angle also affect ACDR performance. Small-scale experiments showed that maximum cavity length occurred at an optimum hull position and diminished rapidly with any variations [18]. Positive trim (bow up) conditions limit downstream cavity growth due to an adverse pressure gradient, while negative trim (bow down) conditions increase air leakage from the cavity tail and tend to disintegrate the cavity front portion. Initial experiments with larger air-cavity hull models indicated that

proper placement of a hydrofoil under the hull can produce elongations of the air cavity at significant positive and negative trim angles [19].

The liquid-gas interactions important for air-cavity systems on ships are also of practical interest for other applications. For example, air entrainment affects the performance of stepped spillways that dissipate flow energy near dams to prevent structural damage [20]. The simultaneous flow of gas and liquid inside pipes can cause the formation of liquid "slugs" that make the flow highly unstable and can cause significant damage to facilities [21]. Physical complexity of multiphase flows makes it difficult to model and accurately predict these scenarios, while even the most detailed empirical data is typically useful within a narrow range of experimental parameters [22]. Due to limitations in multi-phase theoretical analysis, improvements in air cavity ship design will require a broad set of experimental data to address more specific conditions likely to be encountered during practical applications.

The main purpose of this study is to experimentally demonstrate the use of stern spoilers, trimmed plates in the front of the recess, and hydrofoils, referred to here as hydrodynamic actuators, for influencing the air-cavity properties on a small-scale simplified hull model.

2. EXPERIMENTAL SETUP AND PROCEDURE

Experiments were conducted in a recirculating open-surface water channel at Washington State

University. Fig. 3 shows schematics of the apparatus and test section dimensions. Two pumps operate at
constant power to drive water flow through the channel, with recirculation valves controlling velocity in
the test section. Fluctuations in water velocity were less than 2% in previous tests performed at this
facility [23]. Maximum speed in the test section of this facility with water depth at 31 cm is 47 cm/s.

The model-scale air-cavity hull was constructed from acrylic plates to provide a clear view inside of the air cavity recess; and it was held rigidly in the test section by an aluminum frame (Fig. 4). Fig. 5a shows a side view hull schematic, with the recess region highlighted in grey. Important dimensions are shown in Fig. 5b. The width of the recess region is 7.5 cm, which is open on the bottom and closed on the sides, whereas the entire hull beam is 8.1 cm. The hull form geometry is mainly two-dimensional, with the exception of the side plates. During the tests no significant variations of the cavity shape in the transverse direction were noticed, except for air leakage which happened in the form of air bubbles or pockets that had dimensions smaller than the recess width.

Due to finite dimensions of the water channel, there is a blockage effect that increases the incident flow velocity on the hull. Using correlations given in [24], it is estimated that the effective incident water velocities were about 1.8% higher than the measured channel velocities. Another restriction effect is due to a finite ratio of the channel water depth to the cavity length. Using results reported in [25], the finite-depth influence on the cavity length in the present setup was estimated to be below 0.5%.

In the front part of the recess, a flat plate along base of the hull can be trimmed by raising or lowering its trailing edge to alter the oncoming water flow (Fig. 5). The rear portion of the recess ceiling gradually slopes downward to form a "beach" that slows downstream air leakage from the cavity. At the stern, a spoiler can be lowered to form an additional barrier to downstream air leakage.

A hydrofoil was mounted below the bottom of the hull with adjustable position and angle of attack. The hydrofoil was a modified E603 profile with its rear section thickened for ease of manufacturing and mounting. Side struts that secured the foil's position and attack angle had rounded edges to minimize their impact on water flow. Both the foil and struts were 3D printed from PLA material. An angle indicator with tick marks at -10°, 0°, and +10° was attached to the struts along the foil's chord line to reference its attack angle in relation to the hull.

Airflow was supplied by a portable air compressor and measured using an Omega FL-1472-G rotameter with a maximum reading of 1.60 standard cubic centimeters per second (sccs). Total uncertainty of mean airflow measurements was 0.084 sccs. Air cavity length and thickness were measured using a transparent measuring grid imprinted with 0.64 cm squares attached outside of the recess region. Hull trim was measured using a digital angle finder with a resolution of 0.1°. Due to some variability in the mounting apparatus, trim angles could only be reproduced within 0.1° of the target value.

Although drag reduction is the primary function of air-cavity systems on ships, drag force or its variations were not measured in the present experimental setup with a rigid supporting structure. The main objective was to investigate the influence of static hydrodynamic actuators on steady-state geometric properties of the air cavity.

Due to a large number of potential variables including water speeds, air injection rates, and actuator deployment states, determining the test matrix required eliminating variables that showed little to no influence on air cavity behavior in the present setup. Actuator effects on the cavity increase with water speed, hence the channel's maximum velocity (47 cm/s) was chosen along with a lower water speed (36 cm/s) that can be reliably maintained. Based on the air-cavity recess length and water properties, these water speeds correspond to Reynolds numbers of 1.4·10⁵ and 1.1·10⁵ with Froude numbers of 0.28 and 0.21, respectively.

Air injection rates between 0.32 sccs and 1.60 sccs were considered, similar to the rates employed in previous studies [18], but steady-state cavity dimensions showed rather small sensitivity to air injection rate at extreme trim conditions, which were of primary interest in this study. Subsequent testing was performed at a constant air injection rate of 0.64 sccs.

Step submergence depth, d (Fig. 5d), was initially varied from 1.9 cm to 5.75 cm at the leading edge of the recess region but showed minimal effects on cavity size. All subsequent testing was performed at

5.75 cm submergence. Hydrofoil depth was held constant at 0.32 cm below the hull, which was close enough to the air-water interface to provide significant influence while allowing a $\pm 10^{\circ}$ range of motion for the foil. Spoiler effects on the air cavity showed no significant change beyond a spoiler deployment depth of 1 cm, nor did front plate adjustments greater than ± 0.8 cm at its trailing edge.

The test campaign included measurements of cavity length L_c and frontal cavity thickness t_c in response to parametric variation of the hull trim angle τ , foil location L_f , and foil attack angle α , in conjunction with previously identified states for other actuators (Fig. 5c,d). Fig. 6 illustrates the definitions of L_c and t_c in two situations. When a long continuous air cavity is present (as shown in Fig. 6a), the cavity length L_c is defined as the horizontal distance between the trailing edge of the front plate and the point where the cavity reattaches to the hull surface, whereas the cavity frontal thickness t_c is the vertical distance between the ceiling leading edge and the air-water interface underneath. In some other conditions, the air cavity under the ceiling splits into two distinct air pockets (as shown in Fig. 6b), with the front part of the ceiling being in contact with water. Total air-cavity length L_c is then taken as a sum of the lengths of these two pockets, while the frontal cavity thickness is zero. The cavity length and thickness are presented below in terms of their normalized relations to the recess length L_r and height t_r , respectively (Fig. 5c).

3. EXPERIMENTAL RESULTS

3.1. Baseline setup

Measured cavity dimensions in a baseline setup without actuators are presented in Fig. 7 as a function of the hull trim angle for two air injection rates and two water speeds. The cavity length fluctuations existed in all cases and increased with water speed and at the extreme negative trim. The cavity lengths

reported on the graphs represent average values between maximum and minimum measured lengths $L_{c,max}$ and $L_{c,min}$ at each condition,

$$L_c = 0.5 (L_{c,max} + L_{c,min}). (3)$$

Error bars in Fig. 7 account for both measurement uncertainty in grid resolution ε_r and fluctuations of the cavity boundary ε_f , calculated as

$$\varepsilon_{Lc} = \sqrt{\varepsilon_r^2 + \varepsilon_f^2} \,, \tag{4}$$

where ε_r = 0.32 cm and ε_f is estimated for the cavity length as a half of the fluctuation magnitude, 0.5 $(L_{c,max}-L_{c,min})$. A similar approach is used for estimating uncertainty of the cavity frontal thickness, also shown via error bars in Fig. 7.

With zero hull trim and no deployment of actuators, the air cavity filled the entire recess region at both water speeds at all rates of air injection. The cavity shape was more sensitive to airflow at extreme negative trim and higher water speed. Maximizing air cavity size at low rates of air injection is desirable for the overall economic performance of the system. Therefore, subsequent actuator testing was performed at the lower air supply rate of 0.64 sccs.

In a practical air cavity system, reductions in total cavity length (L_c) or frontal thickness (t_c) can severely diminish drag reduction effects. At extreme positive trim (Fig. 7), the cavity length is reduced by nearly 30% at both water speeds compared to the reference zero-trim condition. Positive hull trim creates an adverse pressure gradient along the cavity due to hydrostatic pressure that limits its total length, similar to previous studies [18]. This prevents air from reaching the hull stern and instead forces air leakage from the front of the cavity under the sidewalls of the recess, as the air layer thickness cannot be contained. In this situation, the side-wise air leakage typically occurred behind the front plate via air pockets of roughly 1 cm³.

At extreme negative trim, the cavity length was reduced by 58% in the worst case, with many scenarios resulting in zero frontal thickness of the air cavity. This condition corresponds to a wetted region on the underside front portion of the recess ceiling, as was also observed in experiments with a larger ship model [19]. A real ship would not achieve significant drag reduction in such a case. Detrimental effects of large negative trim angle increase with water speed. Photographs of the cavity at extreme trim conditions are shown in Fig. 8, with the cavity boundary highlighted for clarity. At U = 47 cm/s and $\tau = -3.5^{\circ}$, a wetted region formed on the mid-section of the recess ceiling breaking the cavity into two discreet pockets (visible in Fig. 8) and reducing its total length by 58%. In this condition, the forward cavity portion oscillated in size as air pockets migrated downstream to the rear segment and past the hull stern.

Reducing the water speed to U=36 cm/s allowed the cavity length to remain stable down to trim $\tau=-4.0^\circ$, in which case a wetted region appeared near the ceiling leading edge. Air entering the recess was immediately carried downstream to the stable cavity segment without forming a separate region. The difference between wetted zones on the ceiling at two water speeds can be associated with different Froude numbers, which characterize inertia of water flow relative to gravity. At higher speeds, the recirculation zone behind the front plate becomes longer and induces more significant suction on the fluid above, similar to the process occurring behind ship sterns with increasing speed [26]. More pronounced suction at higher speed allows a small air cavity segment to persist under the ceiling front portion.

3.2. Spoiler deployment effects

For the critical negative trim angles at each water speed, deploying the spoiler to a depth of 1 cm below the transom increased the normalized cavity length to near unity. Spoiler effects for improved

conditions are shown in Table 1; and they are more pronounced at higher speeds. At U=47 cm/s and $\tau=-3.5^{\circ}$, the cavity length more than doubled compared to its initial degraded state with no actuators. Photographs of the cavity at both water speeds are shown in Fig. 9. By blocking the oncoming water flow, the spoiler is known to create a high-pressure zone in front of it [27]. This elevated pressure behind the air cavity opposes the downstream air leakage. With positive trim angles, the spoiler had no effect because downstream pressure was already increased by the hydrostatic gradient.

3.3. Front plate deployment effects

The front plate position was regulated by adjusting its trailing edge height by ±8 mm in relation to the bottom of the hull, with negative sign indicating the plate was lowered below the bottom, and positive sign indicating it was raised into the recess region (Fig. 5c). Increasing adjustments in either direction by an additional 1 cm showed no substantial changes. Resulting effects on the cavity length and frontal thickness are compared for both deployment settings and water speeds as a function of the hull trim angle in Fig. 10.

At speed 47 cm/s, raising plate into the recess reduced the frontal thickness for negative trim but did not have significant effects on the total cavity length, except for the most negative trim. Raising the plate at 36 cm/s had minimal impact on cavity thickness but slightly decreased its total length for trim angles below -1.5°. At extreme negative trim, lowering the plate below the base of the hull restored the cavity to its full length at 47 cm/s, an improvement of about 110% compared to the degraded state, which is similar to effects of the spoiler at this speed. At speed 36 cm/s, lowering the front plate was less effective at extreme negative trim and did not fully eliminate forward wetted regions on the recess ceiling. A comparison of cavity images is shown in Fig. 11a,b, illustrating greater effect of the front plate at higher speeds.

Deployment of the front plate altered the direction of the incident water stream, thus changing size of the water recirculation zone behind the plate and the air cavity shape under the ceiling. Deflecting the plate down also enhanced the flow separation zone and lowered pressure near the air entrance. The resulting suction effect [26] was further increased at higher water speeds, and hence was more favorable to the air cavity formation.

At zero and positive hull trim, raising the plate increased cavity length by allowing its leading point to propagate upstream along the plate's lower surface and beyond the confines of the recess region. This condition is shown at +3.5° trim in Fig. 11c. Although upstream growth was favorable for the total cavity length, the closure region also moved slightly upstream and diminished net gains. Lowering the front plate with extreme positive trim was mildly detrimental in most cases, as air leakage under the sidewalls was increased due to the plate trailing edge moving below the side walls.

3.4. Hydrofoil deployment effects

The air-cavity shape showed significant response to variations of the hydrofoil's position and attack angle at both water speeds. Fig. 12 shows a clear optimum foil setting for each condition, yielding a 105% improvement for extreme negative trim at U=47 cm/s when the foil was positioned at $L_f/L_r=-0.02$ (under front plate) regardless of attack angle. Photographs of the improved cavity states at U=47 cm/s and $\tau=-3.5^\circ$ are compared in Fig. 13 at selected foil positions.

A hydrfoil with zero and positive attack angles reduces pressure above its top surface, thus creating a suction effect. This phenomenon was realized in one variation of air-lubrication systems [1], where hydrofoils were employed to deliver air to the hull surface. In another experiment, a hydrofoil under an air cavity helped substantially increase the cavity length [15]. A hydrofoil with negative attack angles produces opposite effects and increase pressure above the foil, which slows flow in that region.

For negative hull trims in this study, hydrofoil benefits quickly diminish as the foil position moves downstream away from the most favorable upstream location; and in many cases the effects are detrimental in comparison with a no-foil setup. However, these effects are non-monotonic (Fig. 12). When located near the recess rear end at $L_f/L_r=0.91$, a hydrofoil with negative attack angles suppresses downstream air leakage by raising pressure behind the cavity, somewhat similar to the spoiler action. The forward wetted region was eliminated in this case. However, the cavity tail was also forced farther upstream. This condition is visible in Fig. 13. At U=36 cm/s with $\tau=-4.0^\circ$ the foil at the rear end was less effective at suppressing downstream air leakage and did not fully eliminate the forward wetted region. At negative hull trim, lowering the water speed reduced the magnitude of foil effects (Fig. 12), hence diminishing its benefit to the air cavity size.

For intermediate values of the relative foil position L_f/L_r at a constant positive attack angle, the non-monotonic cavity responses to foil settings are illustrated in Fig. 14. As L_f/L_r increased beyond its optimal value of -0.02, the forward cavity end was pulled downstream, thus reducing the total cavity length. When L_f/L_r approached the rear cavity segment, the location of the front cavity point shifted either upstream or downstream depending on attack angle. At L_f/L_r greater than 0.56, positive attack angles increased air leakage from the rear cavity segment and further degraded its overall length. Increasing hull trim to +3.5° reduced cavity length significantly at both water speeds due to increasing hydrostatic pressure in the streamwise direction, which inhibited downstream cavity growth. The hydrofoil effectively counteracted this pressure gradient when placed near the closure region in most scenarios, as shown in Fig. 15. At U=47 cm/s, positioning the foil at $L_f/L_r=0.64$ with attack angle +10° increased total cavity length by 24%. For both water speeds, the optimal L_f/L_r position closely corresponded to the closure location L_c/L_r . Previous CFD studies done for a different air-cavity hull

equipped with a foil at the rear end of the cavity indicated a similar effect, as reduced pressure on top of the foil with positive attack angle allowed air to occupy larger recess volume at positive hull trim [19]. Cavity sensitivity to the foil attack angle was rather significant at the optimum L_f/L_r position (Fig. 15). For example, negative attack angles reduced the total cavity length, as illustrated for U = 47 cm/s in Fig. 16. This sensitivity decreased as the foil was shifted upstream (Fig. 15). Moving the foil downstream from its optimal position eliminated all air leakage from under the sidewalls and instead pulled air pockets from the cavity tail past the ship stern. This resulted in a slightly thinner cavity but did not produce significant changes in the total length. Hence, the foil can enhance cavity shapes at positive hull trims, while placing it behind the cavity tail may increase overall air leakage.

6. CONCLUSIONS

Air cavity shapes under a trimmed hull model were experimentally augmented using compact actuators placed at optimal positions. Without actuators, extreme positive trim angles inhibit the downstream cavity growth. These effects were mitigated by deploying a hydrofoil to create a suction zone near the cavity tail, which increased the average air-cavity length by up to 24%. Extreme negative trim angles increase air leakage from the cavity tail and cause wetted regions to develop in the front part of the recess ceiling. In this condition, wetted regions were eliminated by using either a hydrofoil or transom spoiler, which increased the cavity length by up to 110% from its degraded state. Lowering an adjustable plate just upstream of the recess region can also stabilize the cavity at extreme negative trim, but the plate is more effective at higher water speeds. Future research is warranted to measure actual hull resistance and pressure distribution and explore the observed here effects on a larger scale. Greater benefits to the air cavity system may be achieved by varying other geometric and operational parameters, such as the recess length-to-beam ratio, hull form, and speed regimes. Additional research

should also include high-fidelity computational fluid dynamics simulations that can account for a variety of important phenomena, and to determine overall effects of both hydrodynamic actuators and an aircavity system on the ship attitude and drag.

ACKNOWLEDGEMENT

This material is based upon research supported by the U.S. National Science Foundation under Grant No. 1800135.

REFERENCES

- Kumagai I, Takahashi Y and Murai Y. Power-saving device for air bubble generation using a hydrdofoil to reduce ship drag: Theory, experiments, and application to ships. *Ocean Engineering* 2015; 95: 183-194.
- 2. Makiharju SA, Perlin M and Ceccio SL. On the energy economics of air lubrication drag reduction.

 International Journal of Naval Architecture and Ocean Engineering 2012; 4: 412-422.
- 3. Pavlov GA, Yun L, Bliault A and He S-L. *Air Lubricated and Air Cavity Ships: Development, Design and Application*. New York, USA: Springer, 2020.
- 4. Latorre R. Ship hull drag reduction using bottom air injection. *Ocean Engineering* 1997; 24(2): 161-175.
- 5. Murai Y. Frictional drag reduction by bubble injection. *Experiments in Fluids* 2014; 55: 1773.
- Elbing BR, Winkel ES, Lay KA, Ceccio SL, Dowling DR and Perlin M. Bubble-induced skin friction drag reduction and the abrupt transition to air-layer drag reduction. *Journal of Fluid Mechanics* 2008; 612: 201-236.

- 7. Makiharju S, Elbing BR, Wiggins A, Dowling DR, Perlin M and Ceccio SL. Perturbed partial cavity drag reduction at high Reynolds numbers. In: *Proceedings of the 28th Symposium on Naval Hydrodynamics*, Pasadena, CA, USA, 2010.
- 8. Lay KA, Yakushiji R, Makiharju S, Perlin M and Ceccio SL. Partial cavity drag reduction at high Reynolds numbers. *Journal of Ship Research* 2010; 54(2): 109-119.
- 9. Zverkhovskyi O. *Ship drag reduction by air cavities*. Doctoral thesis. Delft, The Netherlands: Technische Universiteit Delft, 2014.
- 10. Butuzov AA. Artificial cavitation flow behind a slender wedge on the lower surface of a horizontal wall. *Fluid Dynamics* 1967; 2(2): 56-58.
- 11. Matveev KI. On the limiting parameters of artificial cavitation. *Ocean Engineering* 2003; 30: 1179-1190.
- 12. Arndt REA, Hambleton WT, Kawakami E and Amromin EL. Creation and maintenance of cavities under horizontal surfaces in steady and gust flows. *ASME Journal of Fluids Engineering* 2009; 313: 111301.
- 13. Shiri A, Leer-Andersen M, Bensow RE and Norrby J. Hydrodynamics of a displacement air cavity ship.

 In: *Proceedings of the 29th Symposium on Naval Hydrodynamics*, Gothenburg, 2012.
- 14. Acosta AJ. Hydrofoil and hydrofoil craft. *Annual Review of Fluid Mechanics* 1973; 5: 161-184.
- 15. Matveev KI and Miller M. Air cavity with variable length under a model hull. *Journal of Engineering* for the Maritime Environment 2011; 225(2): 161-169.
- 16. Karafiath G, Cusanelli D and Lin CW. Stern wedges and stern flaps for improved powering U.S. Navy experience. *SNAME Transactions* 1999; 107: 67-99.

- 17. Vasconcelos JG and Wright SJ. Mechanisms of air pocket entrapment in stormwater storage tunnels.

 In: *Proceedings of ASCE World Environmental and Resources Congress*, Reston, VA, USA, 2006.
- 18. Matveev KI, Burnett TJ and Ockfen AE. Study of air-ventillated cavity under model hull on water surface. *Ocean Engineering* 2009; 36: 930-940.
- 19. Collins JM and Matveev KI. Exploratory tests of hydrofoil influence on air cavity under model boat hull. In: *Proceedings of SNAME Maritime Convention*, Tacoma, WA, USA, 2019.
- 20. Chanson H. Stepped spillway flows and air entrainment. *Canadian Journal of Civil Engineering* 1993; 20: 422-435.
- 21. Bai Y and Bai Q. Subsea Engineering Handbook. Oxford, UK: Elsevier, 2019.
- 22. Brennen CE. Fundamentals of Multiphase Flows. New York, USA: Cambridge University Press, 2005.
- 23. Conger RN. Pressure Measurements on a Pitching Airfoil in a Water Channel. MS Thesis. Pullman, WA, USA: Washington State University, 1992.
- 24. Scott JR. A comparison of four blockage correctors. In: *Proceedings of the 13th International Towing Tank Conference*, Berlin, Germany, 1970.
- 25. Basin AM, Korotkin AI and Kozlov LF. Control of Ship Boundary Layer. Leningrad: Sudostroenie, 1968.
- 26. Doctors LJ. Hydrodynamics of High-Performance Marine Vessels, Volume 1. Charleston, SC, USA:

 CreateSpace, 2015
- 27. Faltinsen OM. *Hydrodynamics of High-Speed Marine Vehicles*. New York: Cambridge University Press, 2005.

Tables

Table 1. Spoiler effects on the air cavity length.

Speed and trim	U = 36 cm/s,	U = 47 cm/s,
	$\tau = -4.0^{\circ}$	$\tau = -3.5^{\circ}$
L _c /L _r , no spoiler	0.76	0.47
L _c /L _r , with spoiler	0.96	0.98
Relative increase of cavity length	27%	110%

Figures

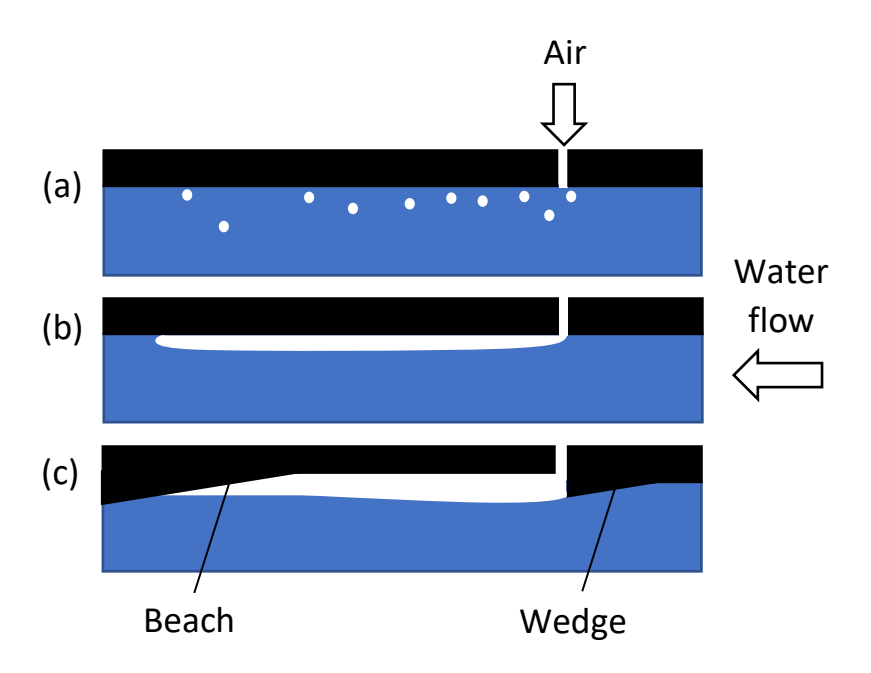


Fig. 1 Air-based drag reduction systems: (a) bubbly flow, (b) thin air layer, (c) air cavity.

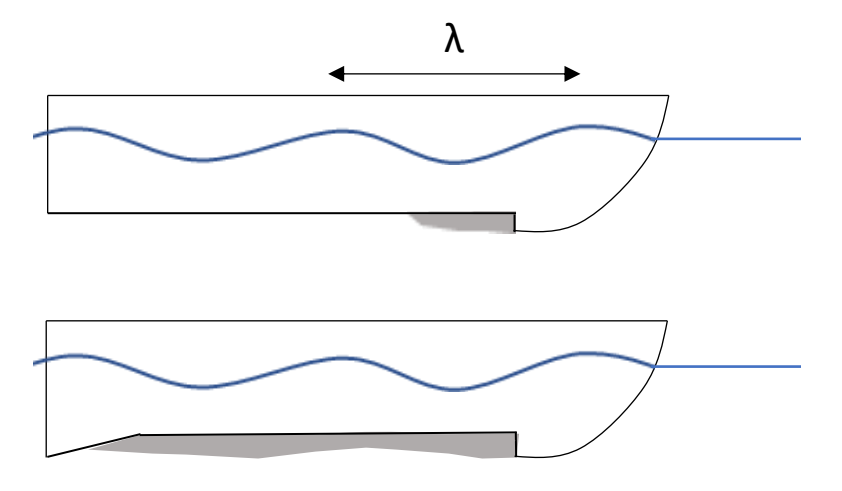


Fig. 2 Air cavity limited by wavelength fraction (top) compared to multi-wave cavity made possible by adding a recess closure (bottom). Air cavity volume is shaded.

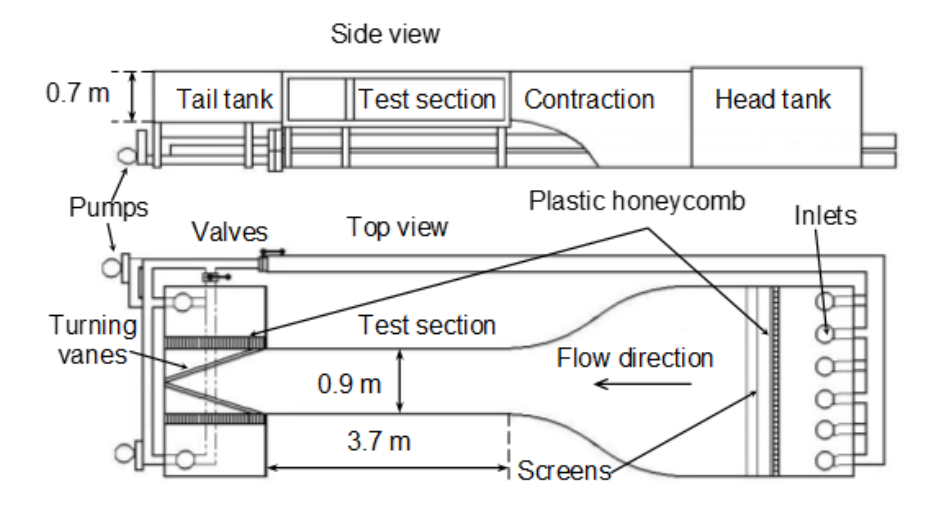


Fig. 3 Water channel features and dimensions.

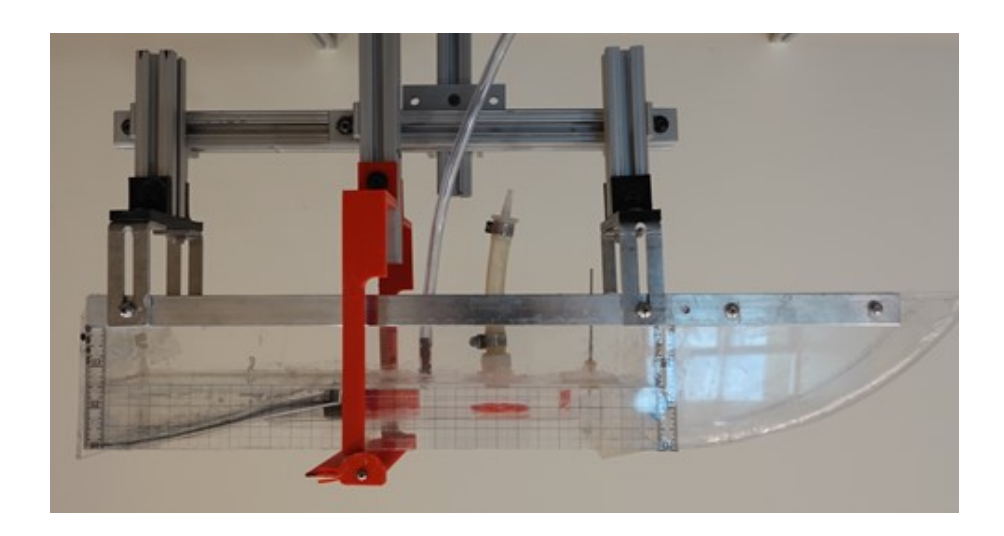


Fig. 4 Photograph of the test model and mount.

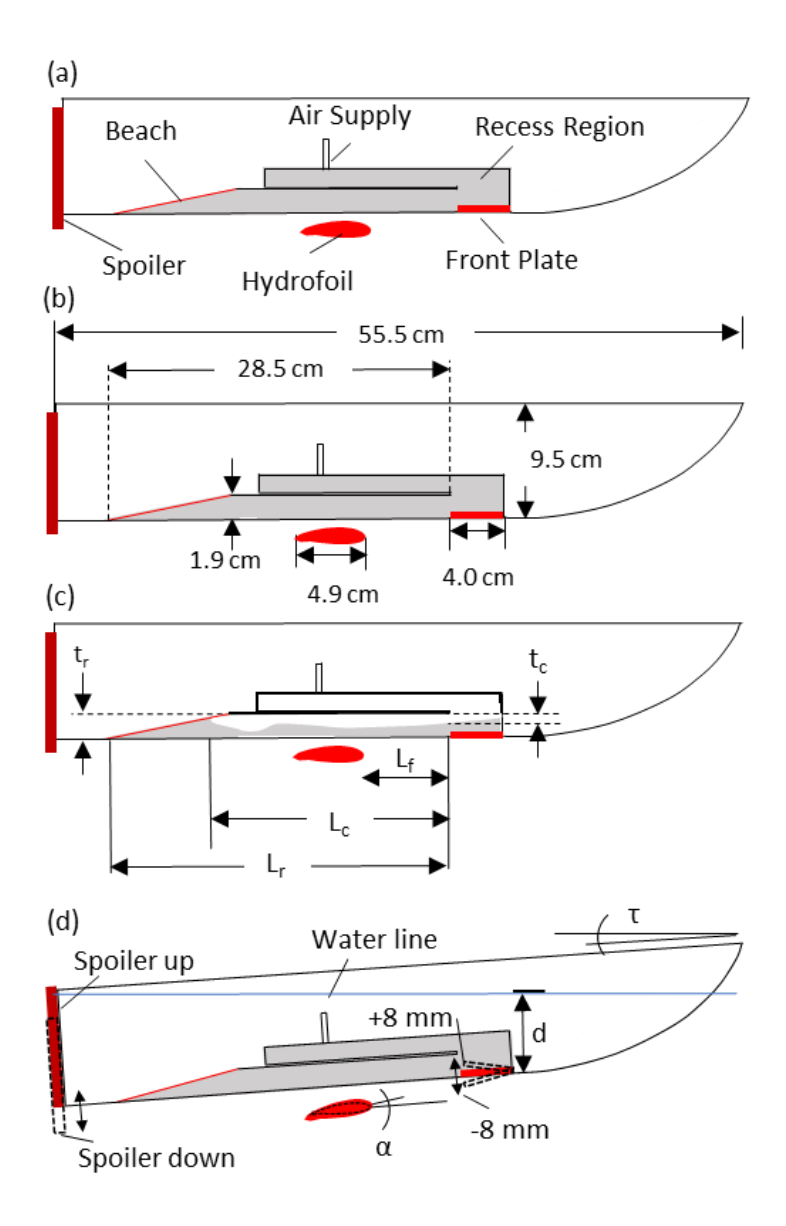


Fig. 5 Model hull dimension and features. Actuators and cavity recess features are labeled in (a).

Relevant dimensions are shown in (b). Sub-figure (c) shows a representative air cavity shape with its features labeled in relation to the recess and hydrofoil locations. Actuator deployments and hull trim are shown in relation to the water line in (d).

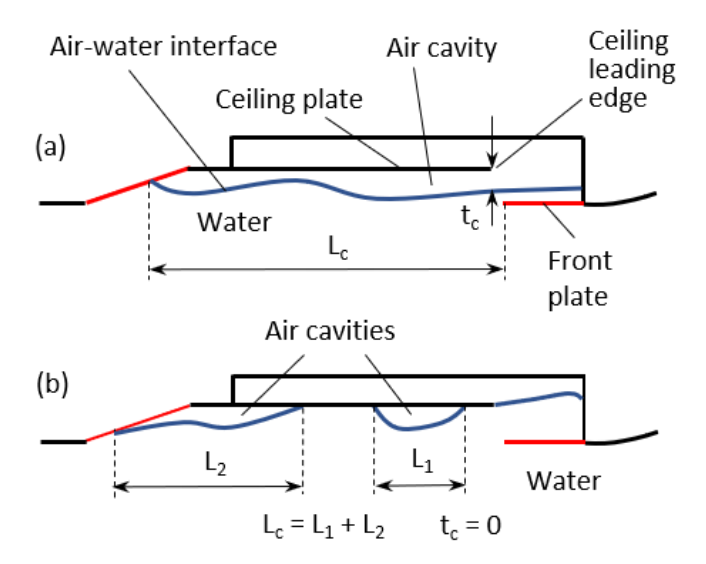


Fig. 6 Definitions of the air-cavity length L_c and frontal thickness t_c for two representative cases: (a) continuous air cavity with finite frontal thickness; (b) two separate air pockets with zero frontal thickness of the air cavity.

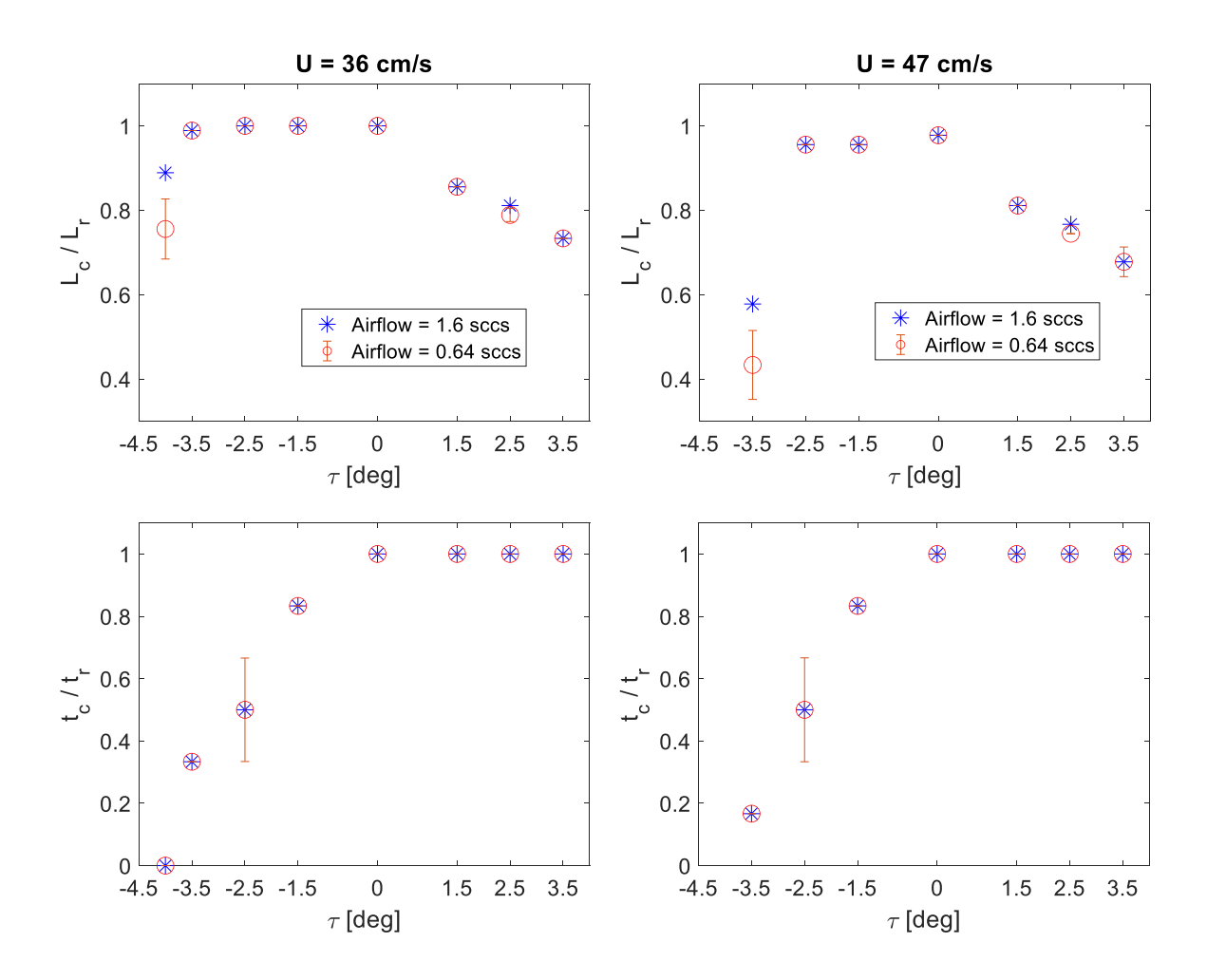
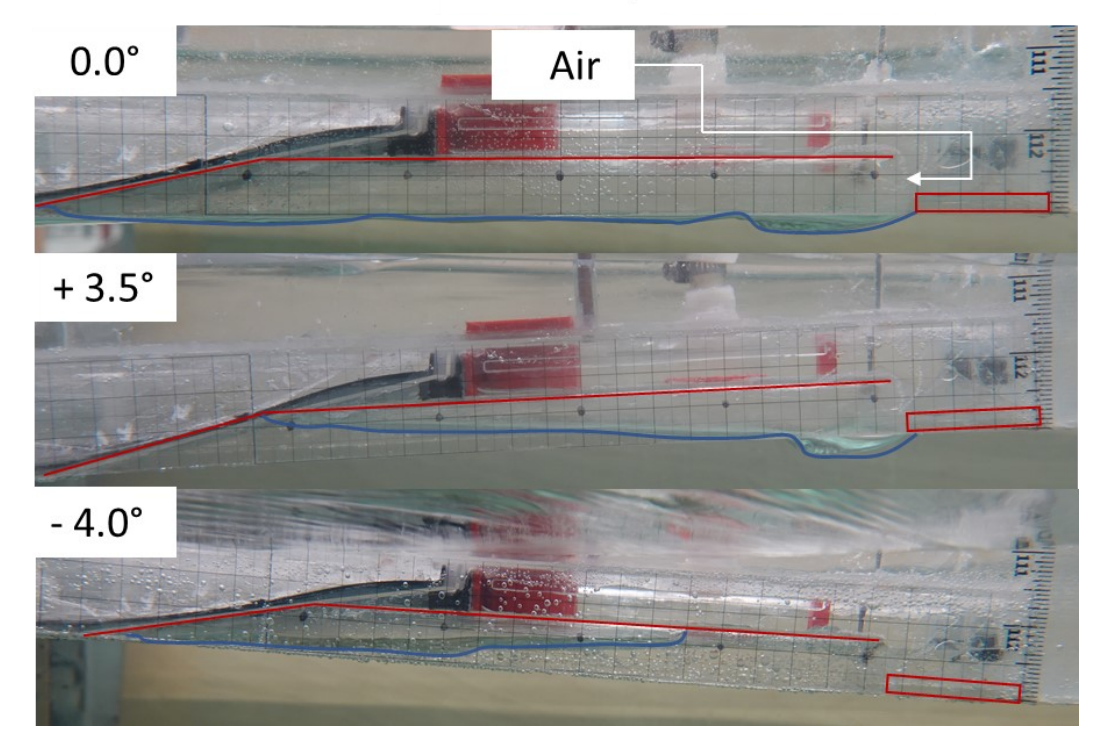


Fig. 7 Cavity dimensions at different trim angles and airflow rates for two water speeds. Only the largest and smallest error bars are shown.

U = 36 cm/s



U = 47 cm/s

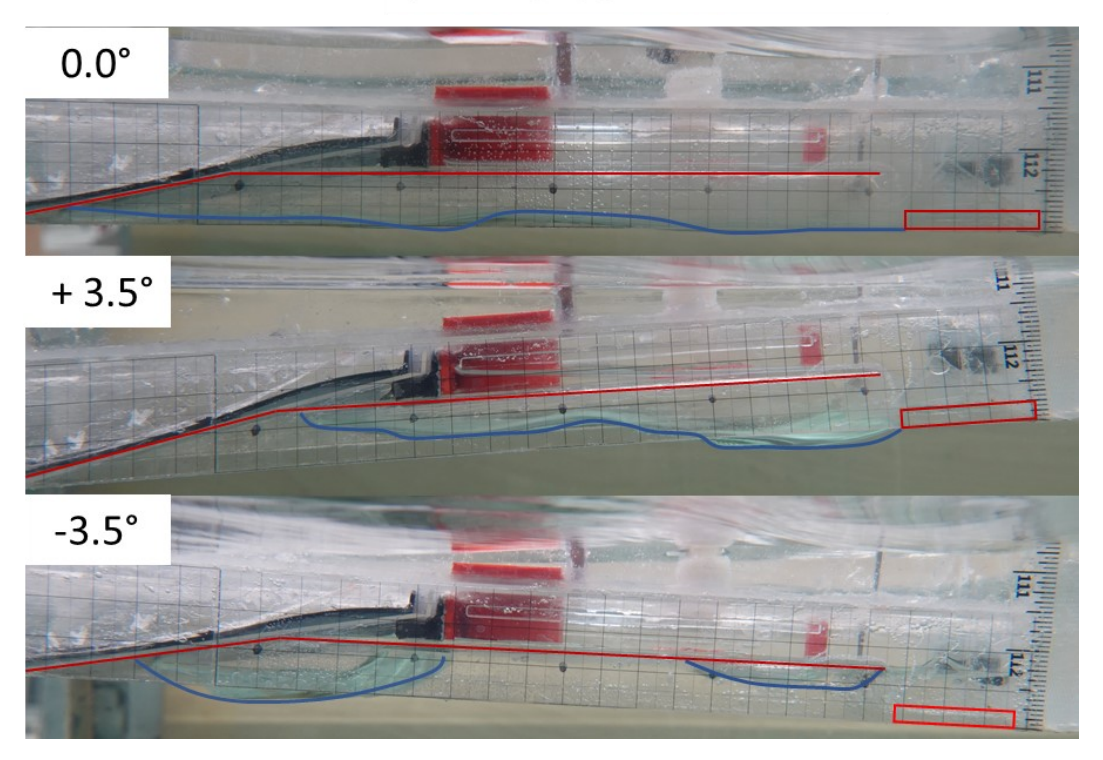
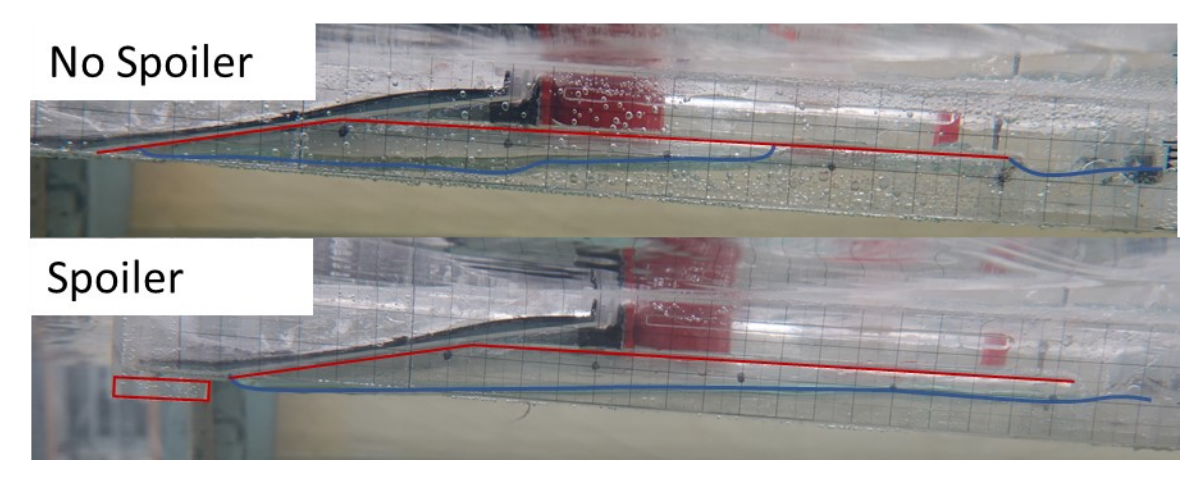


Fig. 8 Cavity shapes at zero and large trim angles and two water speeds. Cavity recess and front plate are colored for clarity. Air-water interfaces are highlighted by curvy lines. Water flow is from right to left.

U = 36 cm/s,
$$\tau$$
 = -4.0°



U = 47 cm/s,
$$\tau$$
= -3.5°

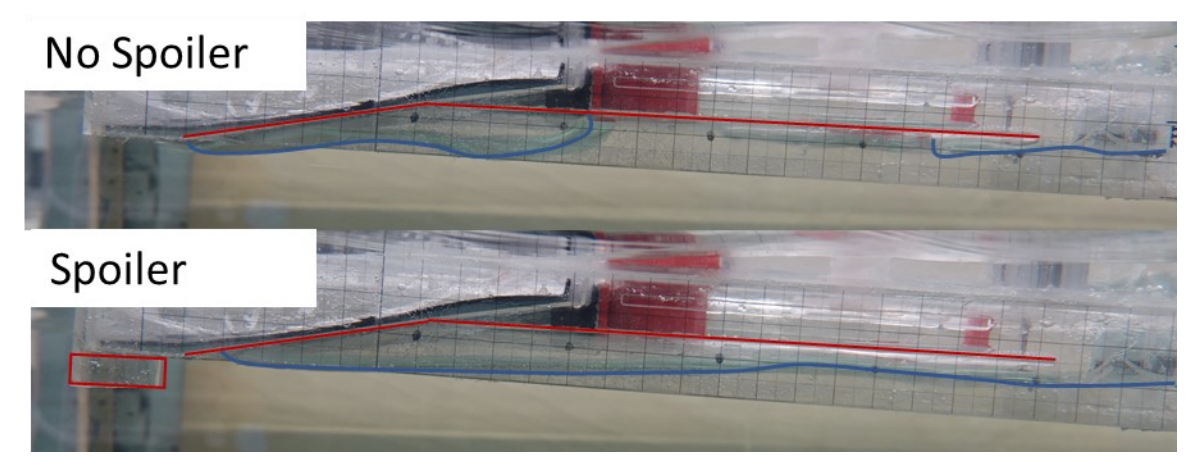


Fig. 9 Spoiler effects for two water speeds at U=36 cm/s and $\tau=-4.0^{\circ}$ (top), U=47 cm/s and $\tau=-3.5^{\circ}$ (bottom). For U=47 cm/s without spoiler deployment, a detached air pocket shed by the front cavity segment migrates downstream toward the rear cavity segment. The rear cavity segment is shown at its maximum length just before an air leakage event. Spoiler is highlighted on the left side. Water flow is from right to left.

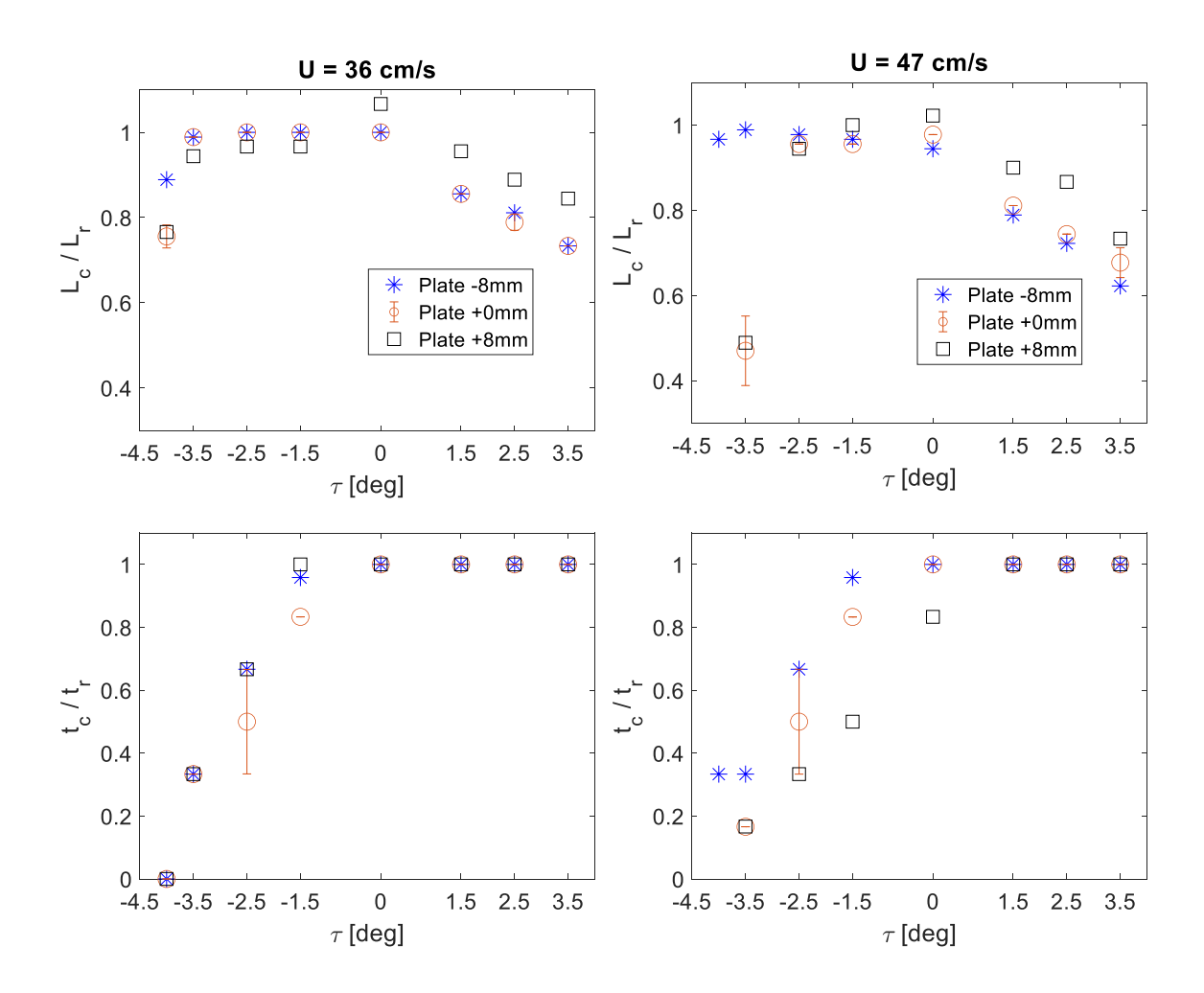
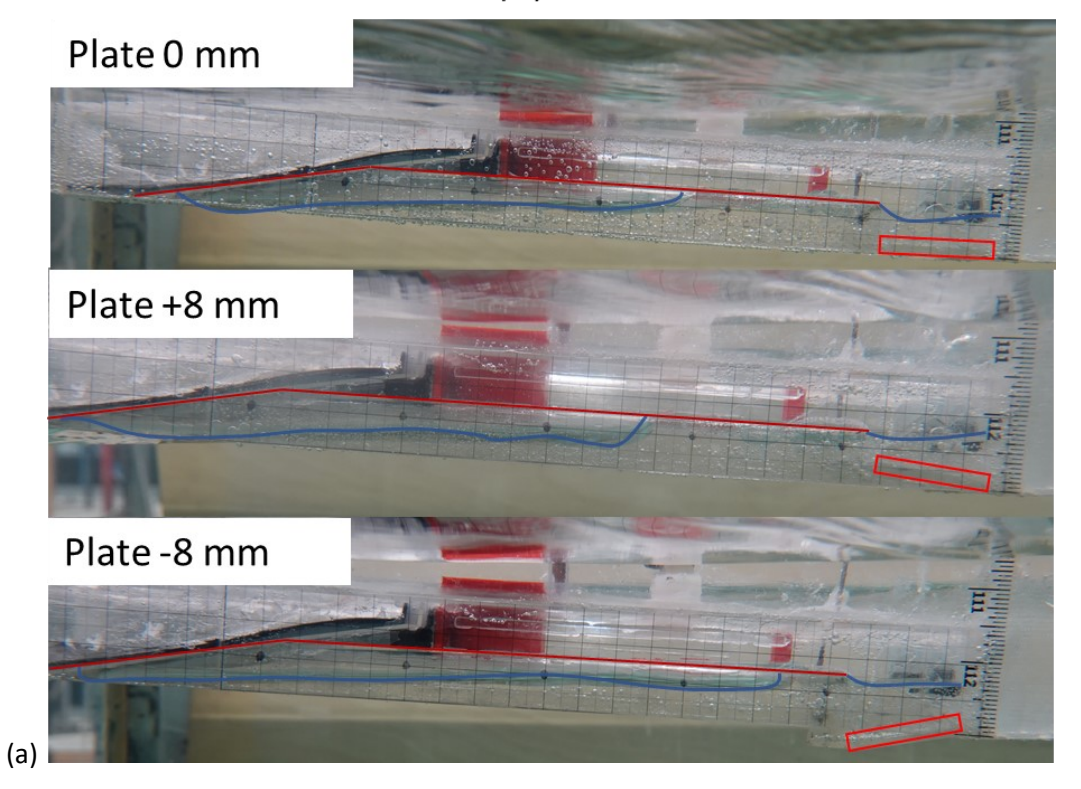
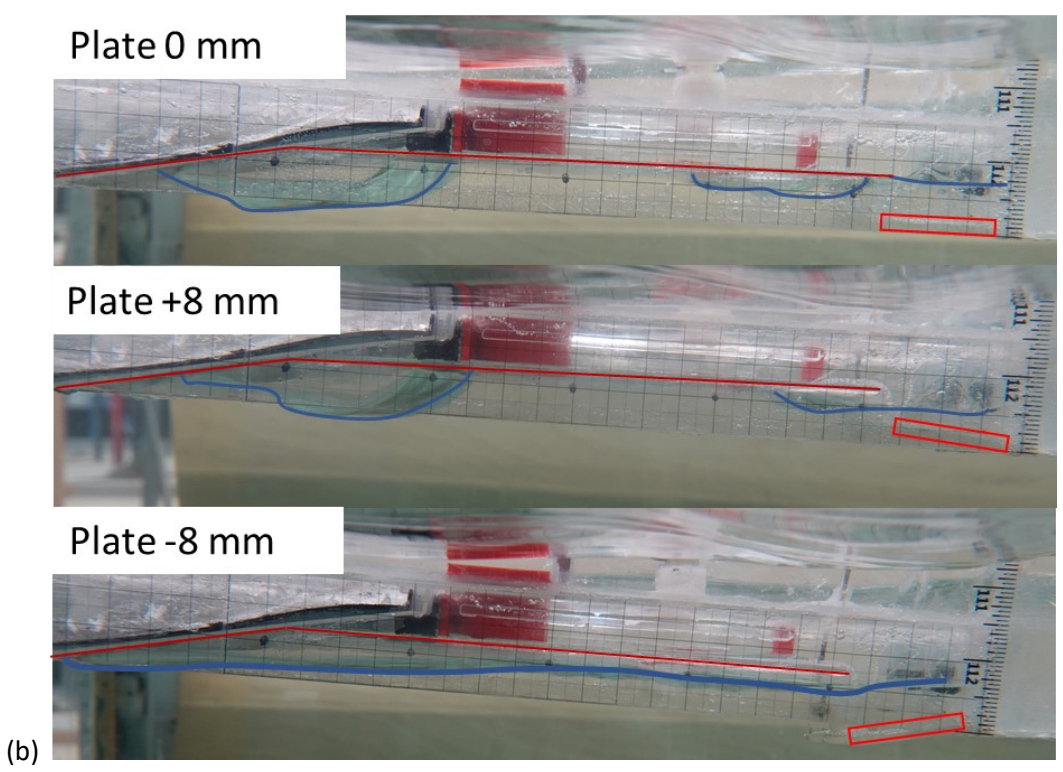


Fig. 10 Effects of front plate position at different hull trim angles. Only the largest and smallest error bars are shown.

U = 36 cm/s, τ = -4.0°



 $U = 47 \text{ cm/s}, \tau = -3.5^{\circ}$



29

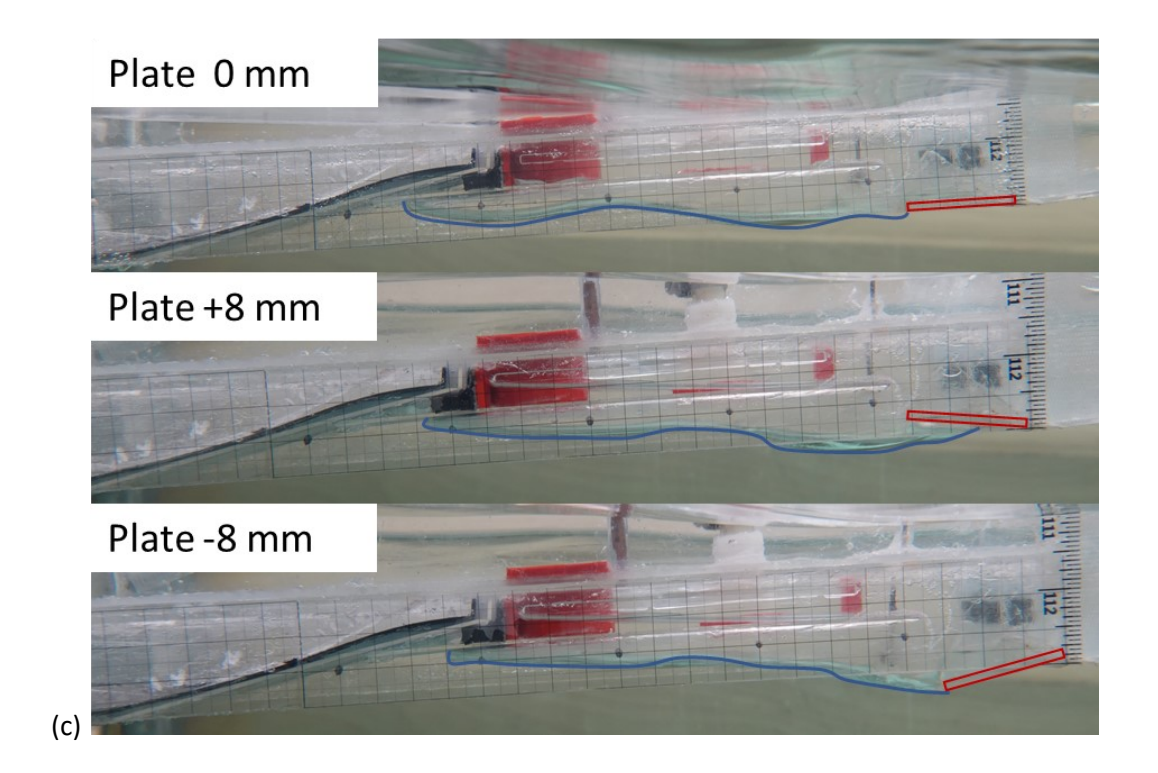


Fig. 11 Front plate effects: (a) U=36 cm/s and $\tau=-4^\circ$, (b) U=47 cm/s and $\tau=-3.5^\circ$, (c) U=36 cm/s and $\tau=+3.5^\circ$.

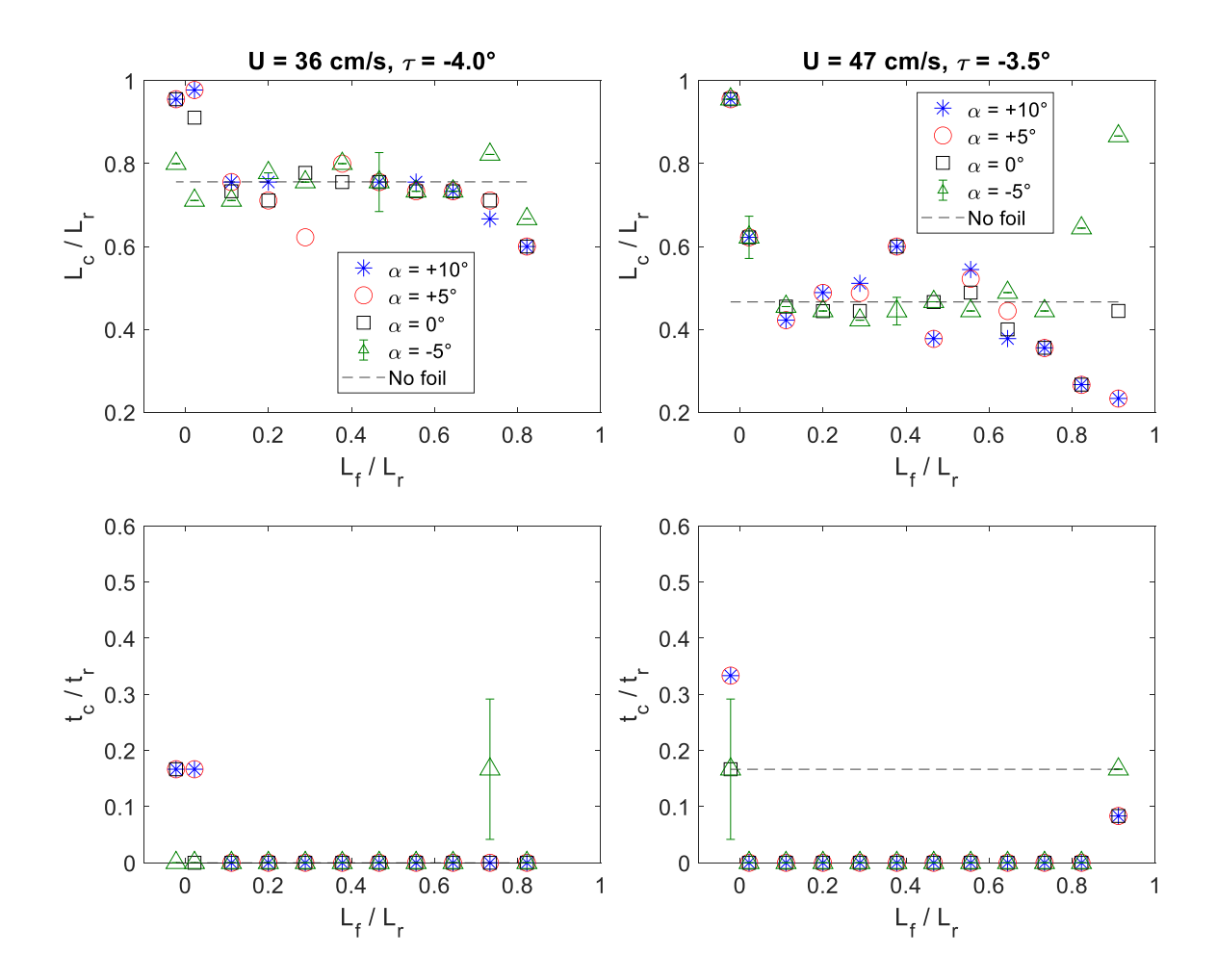


Fig. 12 Hydrofoil effects at negative trim. Dashed horizontal line indicates cavity dimensions with no actuator deployment.

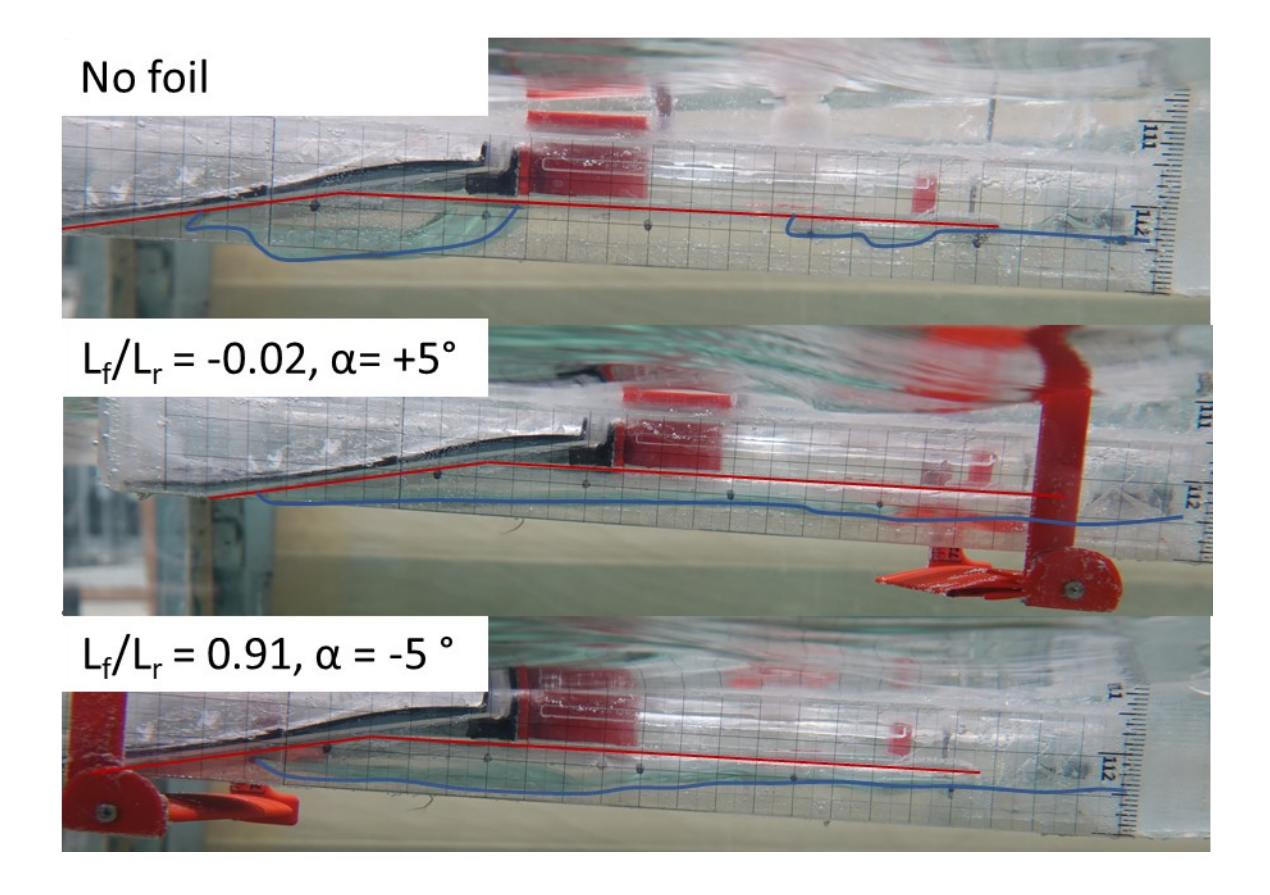


Fig. 13 Comparison of hydrofoil effects at U = 47 cm/s and τ = -3.5°. (Top) no foil, (middle) foil suction allows formation of full cavity, (bottom) foil restores cavity by blocking downstream air leakage.

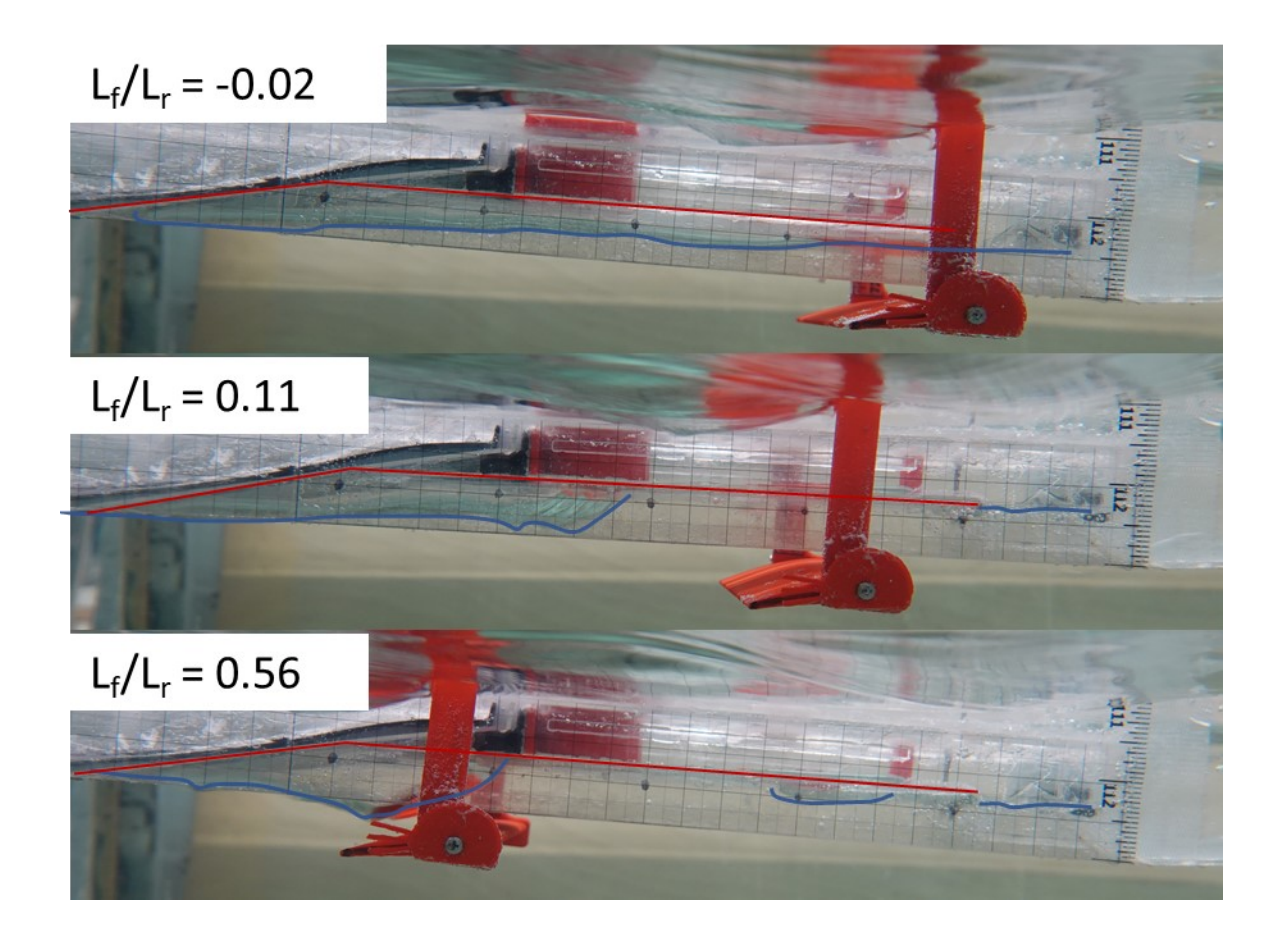


Fig. 14 Cavity shapes at optimal and sub-optimal foil settings with α = +10°. (Top) foil restores cavity and eliminates wetted regions on the ceiling, (middle) forward segment of cavity is pulled downstream by foil, (bottom) forward cavity segment returns, but rear cavity segment is pulled back by the foil.

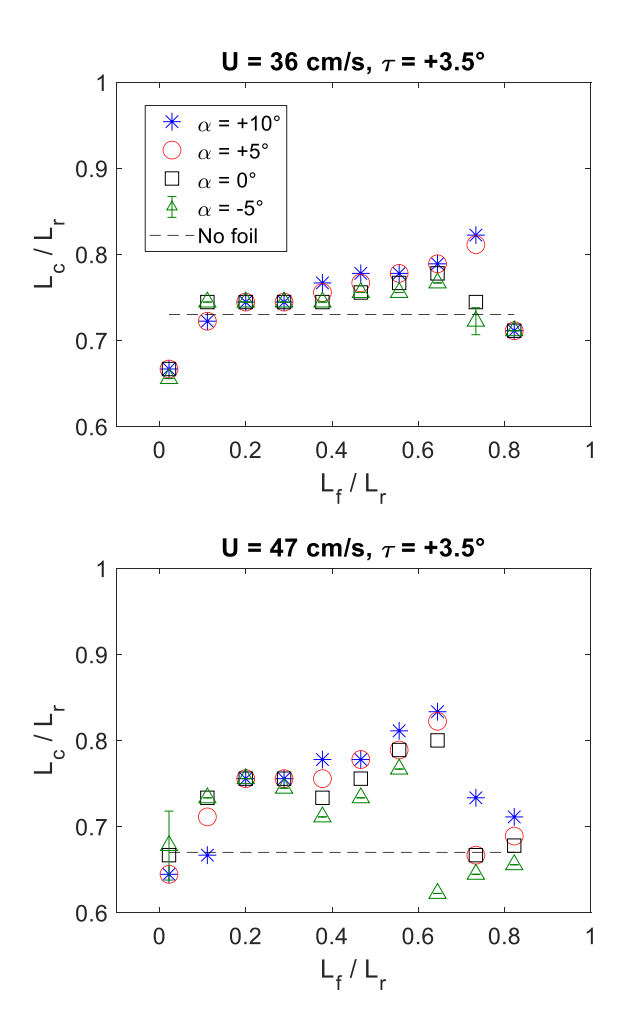


Fig. 15 Hydrofoil effects at +3.5° trim. Dashed horizontal line indicates cavity dimensions with no actuator deployment.

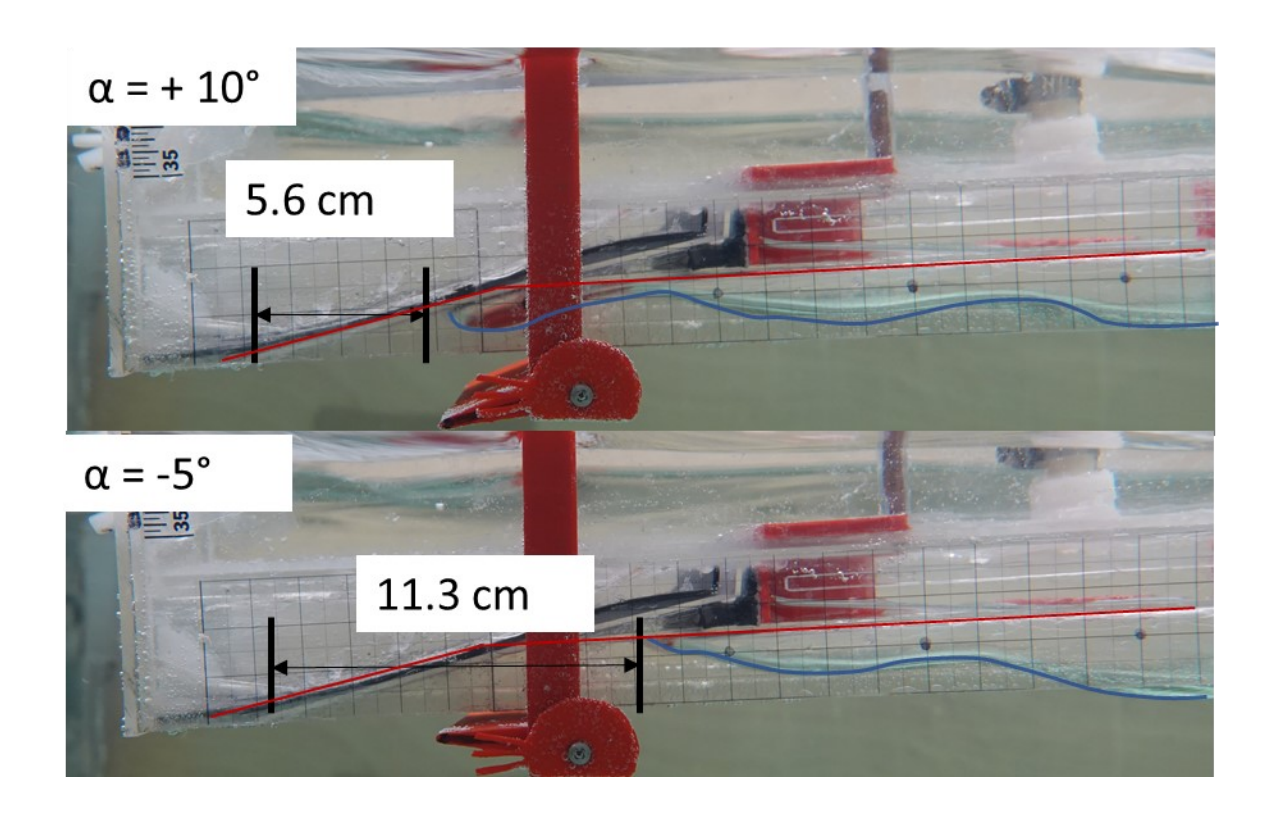


Fig. 16 Change in cavity length with hydrofoil attack angle at τ = +3.5°, U = 47 cm/s, L_f/L_r = 0.64. (Top) foil extends cavity tail with suction generated at positive attack angle, (bottom) foil pushes cavity tail forward by raising pressure at negative attack angle.